

Consider  $1 \text{ m}^2$  of the stellar surface and let it radiate as a perfect blackbody into all directions in the upper hemisphere. Integrate the spectrum over all frequencies and all directions, taking into account the projected area,  $\cos \theta$ , at angle  $\theta$  to obtain the total power radiated by the  $1 \text{ m}^2$ . It turns out to be

$$\Rightarrow \mathcal{F} = \sigma T^4 \quad (\text{W m}^{-2}; \text{blackbody radiation}) \quad (11.25)$$

where  $\sigma$  is the *Stefan–Boltzmann constant*:

$$\sigma = \frac{2\pi^5 k^4}{15 c^2 h^3} = 5.670 \times 10^{-8} \text{ Wm}^{-2} \text{ K}^{-4} \quad (\text{Stefan–Boltzmann constant}) \quad (11.26)$$

The calculated flux (25) is that which passes in one direction through a surface immersed in a blackbody cavity. The total flux (in both directions) through the surface would be zero. The flux (25) increases rapidly with temperature. A doubling of the temperature yields a power greater by a factor of 16.

Since the spectrum from a normal star approximates that of a blackbody, one can use (25) to estimate its luminosity in terms of its surface temperature  $T$  and radius  $R$ . The surface area of the spherical star is  $4\pi R^2$  and its luminosity is  $L \approx 4\pi R^2 \sigma T^4$ . The approximate equality indicates that the star does not emit as a perfect blackbody. In Section 9.4, we defined an *effective temperature*  $T_{\text{eff}}$  (9.13) to yield the exact relation,

$$\Rightarrow L = 4\pi R^2 \sigma T_{\text{eff}}^4 \quad (\text{W}; \text{luminosity of spherical object}) \quad (11.27)$$

The total power  $L$  radiated by a star thus varies as the fourth power of  $T_{\text{eff}}$  and the second power of its radius  $R$ .

Models of normal stars tell us that the more massive stars are both larger and hotter. In a simple model, the luminosity increases extremely fast with temperature, approximately as  $L \propto T_{\text{eff}}^5$  for lower mass stars where the dominant fusion process is initiated by a proton–proton interaction, the *p–p process*. For the massive hotter stars where fusion interactions involving carbon, nitrogen and oxygen take place, the model indicates  $L \propto T^{13}$ . A small rise of surface temperature signifies a huge increase in the output from the thermonuclear reactions that power the star.

### 11.4 Spectral lines

Spectral lines provide powerful diagnostics of the conditions in the emitting region of a celestial source. Normal stars exhibit absorption lines due to decreasing temperature (with altitude) in the photosphere (Fig. 10a) while ejected gas near a star or an active corona can result in emission lines (Fig. 10b). Here we discuss the

several types of spectral lines and their measurable characteristics. In the following section, we present the physics of radiation propagation that creates the lines.

#### Absorption and emission lines

Spectral lines arise from atoms or molecules undergoing transitions between two energy states differing in energy by  $\Delta E$ . Such transitions in the hydrogen atom are shown as arrows in Fig. 10.1. If the atom is going from a high (excited) energy state to a lower energy state, the excess energy is emitted as a photon of energy  $\Delta E = h\nu$ . If many atoms do this, many photons with the same energy are emitted giving rise to an *emission line* (Fig. 1a), provided the photons can emerge without further scatters.

On the other hand, if these atoms are being excited to a higher energy state through the absorption of photons, only those photons of the correct energy,  $\Delta E = h\nu$  will be absorbed. If the absorbing atoms are between us and the source of the original photons (say, a hot star), a deficiency of photons at that frequency, an *absorption line*, will be observed.

Each type of atom or molecule emits or absorbs radiation at frequencies characteristic of that atom; the observed frequencies therefore indicate the type of atom involved. The sodium doublet ( $\lambda \sim 589 \text{ nm}$ ) is one example, and the  $\text{H}\alpha$  line of hydrogen at  $\lambda = 656.2 \text{ nm}$  is another.

The emission and absorption processes are a function not only of the kinds of atoms that are present but also of the conditions of temperature and pressure in which the atoms find themselves. For instance, the hotter stars do not show hydrogen absorption because the hydrogen is entirely ionized. Thus the conditions in the stellar atmosphere are directly indicated by the presence or absence of certain lines. See for example our discussion of the Saha equation in Section 9.4.

#### Origin of spectral lines

Figure 11 shows how the emission and absorption lines arise. A hot incandescent lamp emitting a continuum spectrum illuminates a cool cloud containing sodium (Na) atoms. Three observers analyze the light with a prism; each has a different perspective, and each sees a different spectrum. Each can choose to observe the light emerging from the prism directly by eye (observers A,B) or with the aid of a lens and piece of film (observer C).

Observer A studies the light coming directly from the lamp and sees the continuum spectrum. Observer B studies the light from the cloud and observes the Na doublet in emission. The emission-line spectrum arises from the re-emission of the radiation initially absorbed by the Na atoms. If the gas is sufficiently hot, collisions of the gas atoms will also excite the atoms to produce the lines of interest;

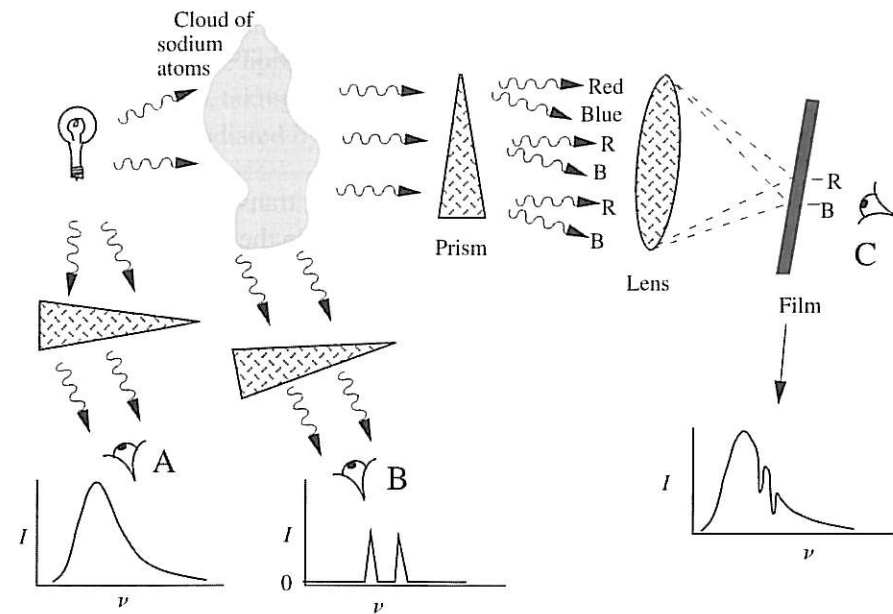


Figure 11.11. Origins of the spectral lines. A continuum source of light illuminates a cloud of sodium (Na) atoms. Three observers, A, B, and C see respectively, the continuum spectrum, emission lines, and the continuum with absorption lines.

the illuminating source need not be present, though it could be the source of the heating. In either case, the characteristic photons are emitted into all directions. Observer C studies the light coming from the direction of the lamp, such that the light has passed through the cloud. The continuum spectrum of the lamp is observed but the sodium atoms have removed many of the photons at the two frequencies of the Na doublet. Thus the doublet is observed in absorption.

In the laboratory there are two classic cases that produce lines. Emission lines are observed from a heated gas such as a Bunsen burner flame, and absorption lines are observed when a cool gas is placed in front of a hot source. The former case is a variant of observer B's situation. The latter is the case of observer C. It is also characteristic of stellar atmospheres which typically exhibit absorption lines.

For the case of observer C, both absorption *and* emission processes along the path from the lamp to observer C must be taken into account. In each differential layer of gas, radiation from the lamp is absorbed at the particular frequencies characteristic of the gas atoms and is diminished as it does so. The atoms in the layer are also emitting radiation characteristic of its cooler temperature. The net spectrum seen by observer C is obtained by integrating these effects layer by layer through the cloud, for each frequency element of the spectrum. The formalism for this *radiative transfer* calculation is presented in the next section.

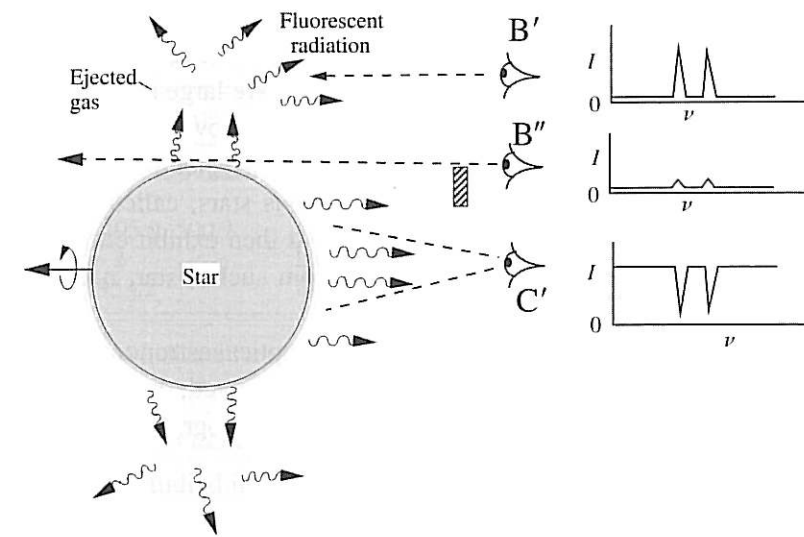


Figure 11.12. Light from a star exhibiting absorption (observer C') and emission lines (B', B''). The view of the stellar disk is blocked for B'' as in a solar eclipse because the chromospheric emission lines seen by B'' are weak compared to the light from the disk. A normal star viewed with no such aid usually exhibits only absorption lines formed in the photosphere, unless large amounts of ejected hot or fluorescing gas are in its vicinity.

#### Stars and nebulae

Radiation from stars exhibits both absorption and emission lines (Fig. 12). When the star is viewed directly, the decreasing temperature with increasing radius in the photosphere results in the production of absorption lines (observer C'). These are known as *Fraunhofer lines* after the discoverer of such lines in the solar spectrum.

Consider now that a large volume of gas is ejected from the star, possibly because the star is rotating so rapidly (see arrow) that centrifugal force ejects part of the atmosphere in the equatorial regions. Photons emitted from the ejected cloud yield emission lines (observer B'). Of course, the star is so distant that an observer on the earth can not distinguish the different parts of the cloud; all the light (and the spectral lines) appear to come from the same place in the sky. Thus, the emission lines must compete with the continuum in the detected spectrum.

Most stars do not have large quantities of ejected gas and thus exhibit only absorption lines (Fig. 10a). A tangential line of sight through the outer layers of a star's atmosphere (chromosphere) does give rise to emission lines, but they are not strong enough to overcome the light from the stellar disk with its absorption lines at the same frequencies. In this case, the emission lines serve to fill in the absorption lines only slightly. Emission lines from the transparent outer layers of

the sun (chromosphere) may be observed by blocking the light from the solar disk, either artificially or with the moon during a solar eclipse (Fig. 12, observer B'').

Stars that do in fact exhibit emission lines must have large amounts of gas that are strongly illuminated by the star or are hot in their own right. Examples are centrifugally ejected gas, an *accretion disk*, an intense *stellar wind*, and a very *active corona*. Massive and hence highly luminous stars, called *luminous blue variables*, can produce major ejections of gas that then exhibit emission lines to distant observers. A portion of the spectrum from such a star,  $\eta$  Carinae, is in Fig. 10b.

Another important example of *emission lines* in optical astronomy is the Balmer radiation emitted from H II regions (Section 10.2). As noted, the prominent hydrogen  $H\alpha$  emission line gives rise to the red regions in photographs of these nebulae.

#### Permitted and forbidden lines

Emission lines that arise from *allowed transitions* are called *permitted lines*. The selection rules of quantum mechanics allow these transitions to occur rapidly. The emitted radiation is *electric-dipole radiation*. If the atom is in an upper state of a permitted transition, the transition will occur after a very short time,  $\sim 10^{-8}$  s.

In contrast, the emission of electric-dipole radiation between certain states of the atom is forbidden by the selection rules of quantum mechanics (angular momentum and parity). These transitions in fact can take place, but with a much lower probability of occurrence. The observed lines are called *forbidden lines*. In such cases, the atom will remain in the upper state for a mean lifetime of order 1 s. The actual mean lifetime depends upon the particular atomic states involved; it is a value between 0.01 s and 100 s for most forbidden transitions. Such a long-lived upper state is called a *metastable state*.

In laboratory situations, even in an excellent vacuum, collision times between atoms will be much shorter than the  $\sim 1$ -s decay time. Thus the metastable states will be *collisionally de-excited* long before they get around to freely radiating a photon. Thus one rarely sees forbidden spectral lines in earth laboratories.

In contrast, the densities within a celestial emission nebula are exceptionally low,  $\sim 10^8$  m<sup>-3</sup>, compared to an excellent laboratory vacuum of  $\sim 10^{14}$  m<sup>-3</sup> ( $10^{-9}$  torr), and collisions occur infrequently. Hence, the atoms in space will often decay via forbidden transitions. (They are excited to the upper states by infrequent collisions with electrons.) In some regions such as the Orion nebula, Fig. 1.7, green light is prominently seen; this is due to emission from two forbidden lines of doubly ionized oxygen, O III, at  $\lambda = 496$  nm and  $\lambda = 501$  nm. Forbidden lines are often indicated with brackets, e.g., the latter line would be designated "[O III] 500.7 nm". The most prominent lines from the Orion nebula are listed in Table 1.

Table 11.1. *Prominent emission lines in Orion nebula*

Wavelength (nm) <sup>a</sup>	Name/color
[O II] 372.61, 372.86	Two ultraviolet lines
H I 486.1	H $\beta$ line, blue
[O III] 495.9, 500.7	Green pair
H I 656.2	H $\alpha$ line, red
[S III] 953.2	Infrared line

<sup>a</sup> Brackets indicate forbidden lines

#### Spectral lines at non-optical frequencies

Spectral lines are studied in all bands from the radio through gamma-ray. In radio astronomy, the study of line emission and the Doppler shifts in frequency of these lines has provided valuable information about the existence of molecules in space (Fig. 13) which are the building blocks of life. The Doppler shifts of "21-cm" spectral lines from the hyperfine (spin flip) transition of hydrogen (Fig. 10.1) reveal the revolution of stars and gas about the center of the Galaxy.

In x-ray astronomy, as noted in the previous section, high-resolution spectra of supernova remnants reveal the heavy elements ejected in the explosion (Fig. 5a). Observations of stellar coronae similarly reveal the elements therein (Fig. 5b). In general, x-ray line studies of Fe (iron) and other elements provide diagnostics of temperatures and densities of the hot ( $T \approx 10^7$  K) plasmas in the source regions.

#### Line strengths and shapes

##### Equivalent width

A typical spectral line will have a *profile* that may be more or less Gaussian in shape and which can be severely distorted under certain conditions (Fig. 14). The total (integrated) area of an absorption or emission line in the observed spectrum is the measure of its strength or total power. The irregular shape of some lines makes it useful to define a quantity that is a measure of this integrated power relative to the other light from the star.

This quantity is called the *equivalent width* (EW). The EW is defined as the width (in wavelength or frequency) of the nearby continuum flux that contains the *same power* (same area on the plot) as the real line, that is, the dark shaded areas in Fig. 14. A large EW means the line is quite pronounced compared to the continuum flux. In



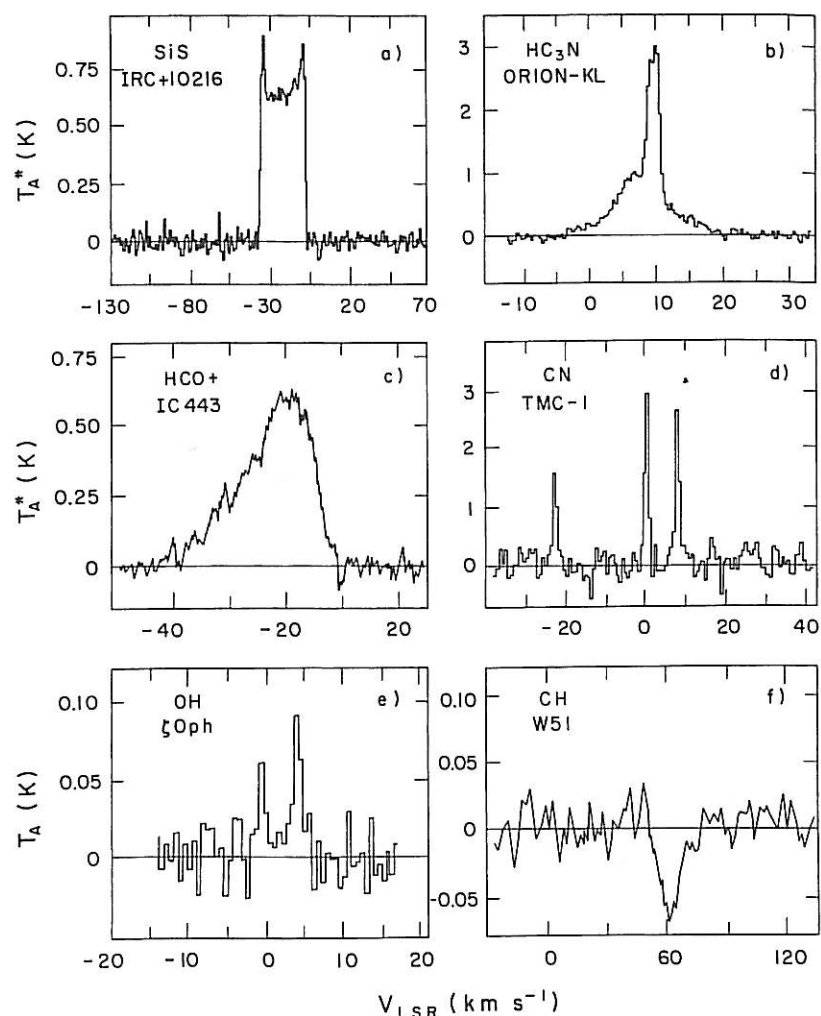


Figure 11.13. Sample radio spectra showing molecular lines from different sources. The objects are (a) late-type carbon star, (b) active molecular cloud core region, (c) a supernova remnant, (d) dark cloud core, (e) diffuse cloud, (f) giant molecular cloud. The observed lines are identified as being specific lines in SiS, CN, etc., so their rest frequencies are known. The abscissa indicates the radial Doppler velocity that is associated with a given observed frequency for the specified line. These plots thus give directly the radial velocities of the emitting clouds. [From B. Turner & M. Ziurys, in *Galactic and Extragalactic Radio Astronomy*, eds. G. Verschuur and K. Kellermann, 2nd Ed. Springer, 1988, p. 210]

the case of absorption (Fig. 14a,c), this hypothetical (dark-shaded) line has total absorption over the equivalent width. For emission (Fig. 14b,d), the equivalent width can be extremely large if the line is intense and the continuum is very small; it will be infinite if there is no continuum flux!

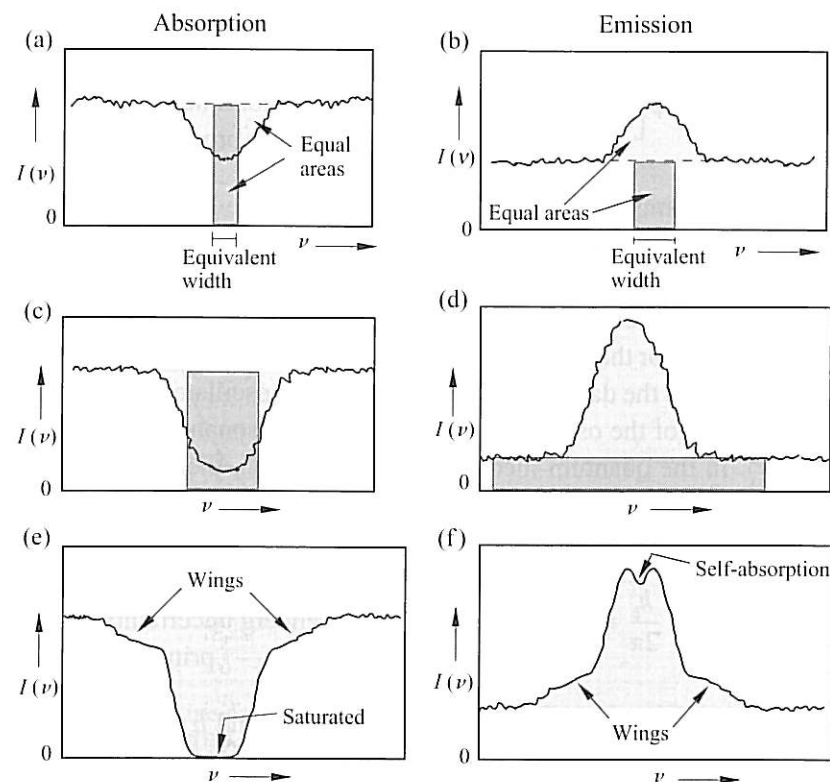


Figure 11.14. Rough sketches of hypothetical spectra for weak lines (a,b), moderately strong lines (c,d), and intense lines (e,f). The concept of equivalent width EW is illustrated in (a-d). The weak wings due to pressure broadening become prominent for the more intense lines. The emitting cloud can begin to absorb its own radiation if it is sufficiently dense (f).

#### Damping and thermal profiles

The profile of a spectral line from a sample of unperturbed gas has a shape governed primarily by two factors. First, the atoms in the gas will have a thermal spectrum governed by the Maxwell-Boltzmann (M-B) velocity distribution. The atoms are receding from and approaching the observer; radiation emitted or absorbed by them will be shifted in frequency due to the Doppler shift. This broadens the lines because both red and blue shifts are present. The Doppler shift of the frequency is proportional to the velocity component along the line of sight. The M-B distribution gives the number of atoms at each speed. Thus the line shape is governed by the M-B distribution; this is called *thermal Doppler broadening*, or simply, *thermal broadening*.

The M-B distribution is a Gaussian (or normal) distribution of speeds (6.3). The speeds translate directly to a Gaussian distribution for the line shape, that is, the

line amplitude  $\kappa_1(\nu)$  vs. frequency  $\nu$ . For an emission line,

$$\frac{\kappa_1}{\kappa_{1,0}} = \exp\left[-\frac{(\nu - \nu_0)^2}{2\sigma^2}\right] \quad \text{(Emission line shape; Doppler broadening)} \quad (11.28)$$

where  $\kappa_{1,0}$  is the amplitude at  $\nu = \nu_0$ , where  $\nu_0$  is the central frequency of the line, and where  $\sigma$  is the standard deviation (characteristic width) of the Gaussian (6.3). The parameter  $\kappa_1$  represents the frequency dependent opacity ( $\text{m}^2/\text{kg}$ ). We explore the connection between spectral lines and opacity in the next section.

The second factor that broadens the spectral line is known as the *damping profile*. Classically, this is the damping term of the classical oscillator. Friction or radiation shortens the life of the oscillator and broadens the resonance curve (amplitude vs. frequency). In the quantum-mechanical interpretation, the limited lifetime  $\Delta t$  of the initial state leads to an uncertainty  $\Delta E$  in the energy of that state, according to the *Heisenberg uncertainty principle*,

$$\Delta E \Delta t \gtrsim \frac{h}{2\pi} \equiv \hbar \quad \text{(Heisenberg uncertainty principle)} \quad (11.29)$$

where  $\Delta t$  is the time the atom is in the upper state and  $h$  is the Planck constant. The longer the atom is in the state, the more precisely its energy can be measured. A large *transition probability* leads to a short life in the state and a large energy uncertainty. The emitted (or absorbed) photons thus yield a broadened line shape.

The expected damping line profile obeys the classical formula,

$$\frac{\kappa_2}{\kappa_{2,0}} = \frac{\gamma}{(\nu - \nu_0)^2 + (\gamma/2)^2} \quad \text{(Damping curve)} \quad (11.30)$$

where  $\gamma$  is the full width at half the maximum height of the line profile and  $\kappa_{2,0}$  is an adjustable amplitude factor. It turns out that  $\gamma$  is proportional to the transition probability (not shown here). A large transition probability, i.e., a shorter lifetime, thus corresponds to a wider profile, or energy uncertainty, as expected.

The line shapes for the two effects (damping and thermal broadening) are shown in Fig. 15 for the case where the width at half maximum of the damping curve is half that of the thermal curve. In stellar atmospheres the central portion of the damping profile is quite narrow. Thus one might expect that the damping would not be important. But the exponential in (28) drives the thermal term strongly toward zero as one moves off center, and the damping curve dominates in the wings.

The combined thermal/damping line profile can be visualized in the following manner. Consider that each moving atom emits photons with the narrow damping profile centered on the Doppler-shifted line frequency  $\nu'$  of that particular atom,

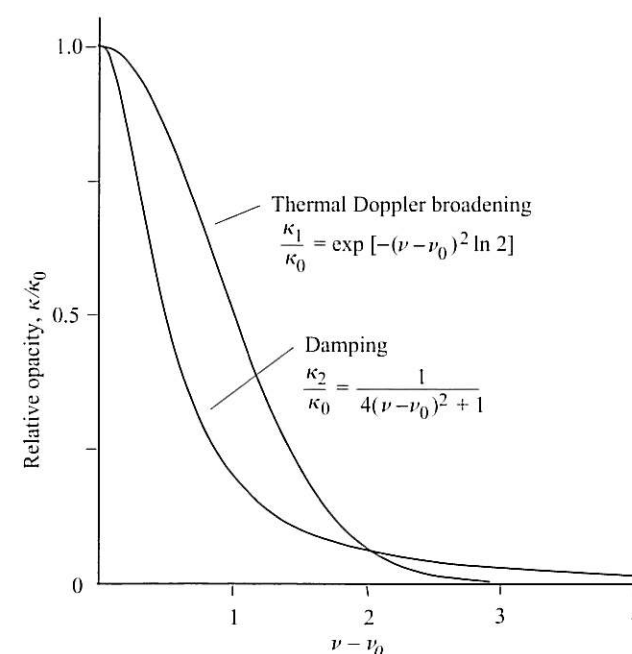


Figure 11.15. Line profiles due separately to the thermal and the damping terms, from (28) and (30) respectively. The opacity  $\kappa$  is plotted against frequency offset from the line center ( $\nu - \nu_0$ ). Both curves are normalized to unity at  $\nu = \nu_0$ , and the widths at half maximum are set to 1.0 and 0.5 for the thermal and damping curves, respectively. Note how the wings of the damping curve dominate at large offsets from the line center.

$$\kappa_2'(\nu) \propto \frac{\gamma}{(\nu - \nu')^2 + (\gamma/2)^2} \quad (11.31)$$

Summation over all atoms (that is, over all Doppler velocities) is a summation of many such profiles centered on the various frequencies  $\nu'$  of the thermal distribution. This smears the two distributions together.

Formally, the damping function  $\kappa_2'(\nu)$  is weighted with the amplitude  $\kappa_1(\nu')$  of the thermal distribution at frequency  $\nu'$  and then integrated over all  $\nu'$ . The net profile  $f(\nu)$  is thus

$$\Rightarrow f(\nu) \propto \int_{-\infty}^{+\infty} \left[ \frac{\gamma}{(\nu - \nu')^2 + (\gamma/2)^2} \times \exp\left(-\frac{(\nu' - \nu_0)^2}{2\sigma^2}\right) \right] d\nu' \quad \text{(Combined profile)} \quad (11.32)$$

which is called the *convolution* of the two functions. When the central part of the damping profile is narrow, the convolution simply maps out the central portion of

the thermal curve, while the damping curve is mapped at off-center positions large compared to the thermal width. If the damping width is down by a factor of 100 or 1000, as it sometimes is, the wings will be at such a low level they will not affect the line shape.

#### Turbulent motions and collisional broadening

Lines can also be Doppler broadened by rapid motions of clouds of emitting or absorbing atoms; this is known as *bulk turbulent motion*. The velocities of the several clouds are not necessarily thermally distributed so the shape of the line may differ from that quoted above. Bulk motion will significantly affect the line shapes when the bulk velocities approach or exceed the thermal velocities.

Broadened lines can also arise from collisions between the gas atoms which will de-excite the atoms before they would decay naturally. The atom is in its initial state for even a shorter time than in its unperturbed state, and this further broadens the (quantum-mechanical) damping profile according to (29). The damping profile is thus a measure of the number of collisions and hence of the density of the gas. (The number of collisions varies as particle density squared  $n^2$ .)

In turn, the density  $n$  is related to the pressure in the region where the line is being formed, as  $P = nkT$  where  $k$  is the Boltzmann constant. This relation follows directly from the ideal gas law  $PV = \mu RT$  where  $\mu$  is the number of moles in a sample of volume  $V$  and where  $R (= N_0k)$  is the universal gas constant ( $N_0$  is Avogadro's number). Thus, for gases of about the same temperature, measurement of collisional broadening yields the relative pressures. This turns out to be useful for stellar classification when comparing different stars of the same photospheric temperatures. Thus

$$\text{Collisional broadening} \leftrightarrow \text{Pressure in photosphere } (T \approx \text{constant}) \quad (11.33)$$

Collisional broadening is sometimes called *pressure broadening*.

#### Saturation and the curve of growth

The *curve of growth* (Fig. 16) of a spectral line describes the measured strength (equivalent width, EW) as a function of the number  $N$  of absorbing (or emitting) atoms along the line of sight (atoms/m<sup>2</sup>). Consider the absorption case (Figs. 14a,c,e). When the strength of the line is weak (Fig. 14a), the atoms along the line of sight are so few they block only a small portion of the beam. An increase in the number of atoms removes a proportional amount of radiation so that the curve grows linearly with  $N$ . As more atoms are added, eventually there are sufficient numbers of low velocity atoms to completely absorb the photons near the central frequency. At this point, the specified line is *saturated*, and the addition of more atoms has only a small effect; the EW increases only very slowly with  $N$ .

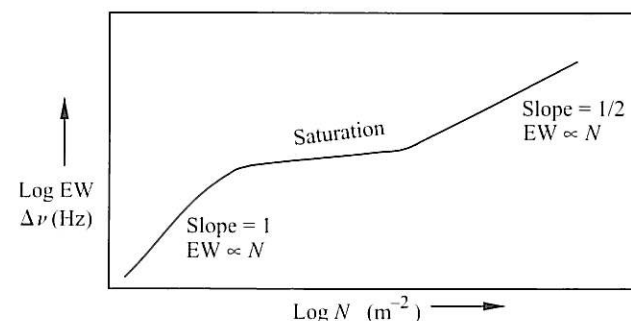


Figure 11.16. The curve of growth or the variation of the equivalent width (EW) with the column density of absorbing atoms  $N$  (atoms/m<sup>2</sup>), for the absorption case. The flattening at intermediate  $N$  is due to the saturation of the central part of the absorption line (Fig. 14e). On this log-log plot, the linear dependence for weak lines and the (approximate) square root dependence for intense lines appear as slopes of 1 and 1/2 respectively.

As more and more atoms are added, the weak wings due to collisional broadening finally become important (Fig. 14e). At this stage the EW begins to increase again, approximately as  $N^{1/2}$ . This is a slower rate of increase in EW than for the unsaturated state. The  $N^{1/2}$  dependence is not derived here. The growth of an emission line (Fig. 14 b,d,f) is largely similar to the absorption case.

The shape of the curve of growth will vary depending on the relative widths of the thermal and damping terms. Knowledge of the curve of growth enables one to determine column densities of different elements in stellar atmospheres and hence the chemical compositions.

### 11.5 Formation of spectral lines (radiative transfer)

Radiation propagating through a gas is transformed by emission and absorption processes. The result is the observed spectrum including spectral lines. Here we set up the differential equation for an elementary case of *radiative transfer* and solve it for several different conditions. This allows us to understand the formation of spectral lines in terms of the frequency dependence of the optical depth.

#### Radiative transfer equation (RTE)

The differential equation that governs the absorption and emission in a layer of gas follows from the geometry of Fig. 17. A uniform cloud ("source") of temperature  $T_s$ , depth  $\lambda$ , and optical depth  $\tau_\lambda$  lies between the observer and a background source at some other temperature  $T_0$ .



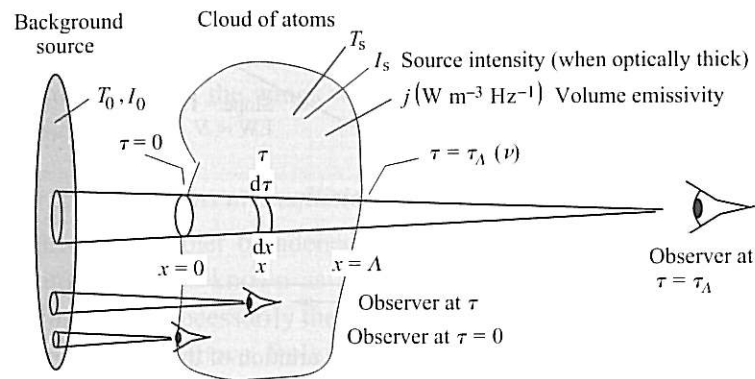


Figure 11.17. Geometry for the radiative transfer equation. The background surface emits with specific intensity  $I_0$  and the intervening gas cloud emits thermal radiation with specific intensity  $I_s$  when it is optically thick. An observer in the cloud at position  $x$ , or optical depth  $\tau$  viewing leftward will detect radiation from the cloud atoms at lesser  $\tau$  and from the background source to the extent it is not absorbed by the cloud.

For the immediate discussion, we refer to radiated intensities at some single frequency (in a differential band) without regard to the entire spectrum. In fact, the overall spectral shape may be inconsistent with a single temperature. Hence we discuss intensities without necessarily defining a temperature. Nevertheless, in stellar atmospheres, temperatures can be defined in regions of *local thermodynamic equilibrium (LTE)*. In this case, a higher intensity at a given frequency does represent a higher temperature.

In the absence of the cloud, the observer in Fig. 17 would detect a specific intensity  $I_0$  ( $\text{W m}^{-2} \text{ Hz}^{-1} \text{ sr}^{-1}$ ) from the background source ( $T_0$ ) at the frequency in question. We refer to  $I_0$  as the *background intensity*. If the intervening cloud is in place, it will absorb some of the radiation from the background source. In addition, the cloud will emit its own thermal radiation in the direction of the observer. If the cloud is optically thick, the emerging radiation would exhibit the specific intensity  $I_s$  characteristic of blackbody radiation at  $T_s$ .

#### Intensity differentials

Consider a beam of photons moving in the direction of an observer at some location in the cloud. The differential equation that describes absorption of the photons in a differential path length  $dx$  is, from (10.17),  $dN/N = -\sigma n dx$ , where  $dN/N$  is the fractional change in the number of photons in the beam,  $\sigma$  ( $\text{m}^2$ ) is the cross section per atom, and  $n$  ( $\text{m}^{-3}$ ) is the number density of atoms. The fractional change of the photon number will be equal to the fractional change in the specific intensity, giving,

$$\frac{dI_1}{I} = -\sigma n dx \quad (\text{Absorption in layer } dx) \quad (11.34)$$

where  $dI_1$  is one of two contributions to the total change  $dI$ .

The cloud also contributes photons to the beam. The thermal emission originating in the layer at  $x$  in  $dx$  of the cloud can be described with the volume emissivity  $j$  ( $\text{W m}^{-3} \text{ Hz}^{-1}$ ). This gives rise to an element of specific intensity from the layer in question which is, from (8.48),

$$dI_2 = \frac{j dx}{4\pi} \quad (\text{Thermal emission from gas}) \quad (11.35)$$

The sum of these two effects yields the net change in intensity  $I$  of the beam,

$$dI = -I\sigma n dx + \frac{j dx}{4\pi} \quad (\text{Net change in } I \text{ in } dx \text{ at } x) \quad (11.36)$$

This is the differential equation that allows us to find, by integration, the variation of beam intensity as it traverses the material on its way to the observer.

#### Intensity variation with optical depth

Rewrite (36) to be a function of optical depth  $\tau$ . Recall the definition of the opacity,  $\kappa \equiv \sigma n / \rho$  (10.24), where  $\rho$  ( $\text{kg/m}^3$ ) is the mass density. Opacity is the cross section per kilogram of material ( $\text{m}^2/\text{kg}$ ). Substitute  $\kappa\rho$  for  $\sigma n$  into (36) and rearrange,

$$\frac{1}{\kappa\rho} \frac{dI}{dx} = -I + \frac{j}{4\pi\kappa\rho} \quad (11.37)$$

The product  $\kappa\rho$  or  $\sigma n$  is simply the inverse of the mean free path  $x_m$  with units of ( $\text{m}^{-1}$ ); see Table 10.1. Thus the product  $\kappa\rho x$  is the *number of mean free paths* in the distance  $x$  for fixed  $\kappa$  and  $\rho$ . In other words it is the *optical depth*  $\tau = \kappa\rho x$ , a dimensionless quantity previously defined (10.29). The denominator  $\kappa\rho dx$  of the left side of (37) is thus equal to  $d\tau$  since  $\kappa$  and  $\rho$  do not change appreciably in an incremental distance  $dx$ .

The equality (37) demands that the rightmost term have units of specific intensity. Since  $j$  is the volume emissivity of our cloud, we define this term to be the cloud intensity, or the *source intensity*  $I_s$ ,

$$I_s \equiv \frac{j (\text{W m}^{-3} \text{ Hz}^{-1})}{4\pi(\text{sr}) \kappa\rho (\text{m}^{-1})} \quad (\text{Source intensity defined: } \text{W m}^{-2} \text{ Hz}^{-1} \text{ sr}^{-1}) \quad (11.38)$$

This expression has the form of (8.53), the relation between  $j$  and  $I$  for an optically thin plasma of thickness  $\Lambda$ , namely  $I = j_{av}\Lambda/4\pi$ . Here, the mean free path  $(\kappa\rho)^{-1}$  plays the role of the cloud thickness  $\Lambda$ . In our optically thick case, an observer can “see” only a depth of about one mean free path into the cloud. The

source intensity (38) is thus the intensity an observer embedded in the cloud would measure if her view were limited by optically thick conditions ( $\tau \gg 1$ ).

It follows from the above considerations that the differential equation (37) may now be written as

$$\Rightarrow \frac{dI(\tau)}{d\tau} = -I(\tau) + I_s \quad \text{(Equation of radiative transfer)} \quad (11.39)$$

where we express  $I$  as a function of  $\tau$ , the optical depth of the cloud in the observer's line of sight (Fig. 17). This is the differential *radiative transfer equation* (RTE) which may be solved for the unknown quantity  $I(\tau)$ , the specific intensity at optical depth  $\tau$  for our chosen frequency.

In (39),  $I(\tau = 1)$  is the specific intensity measured by an observer within the cloud at the depth of one mean free path into the gas. Note that depth is measured from the left edge of the cloud. At  $\tau = 0.1$  or  $\tau = 3$ , the function  $I(\tau)$  is the specific intensity at depths of 0.1 and 3 mean free paths respectively. If the entire cloud has optical depth  $\tau_A$  (corresponding to thickness  $\Delta$ ), the function  $I(\tau_A)$  is the specific intensity measured by the observer outside the cloud.

The quantity  $I(\tau)$  is distinct from  $I_s$ . It includes the radiation from the background source  $I_0$  as modified by absorption and emission in the cloud. The background radiation is the "initial condition" we apply to the differential equation (39). The source function reflects the volume emissivity of the cloud itself.

The quantities  $\tau$ ,  $I(\tau)$  and  $I_s$  in (39) are all functions of frequency; namely  $\tau(\nu)$ ,  $I(\nu)$ , and  $I_s(\nu)$ . We continue to consider one frequency only and suppress the argument  $\nu$ . The function  $j$ , and hence  $I_s$ , can vary with position in the cloud, i.e., both can be functions of  $\tau$ . This is the case in stellar atmospheres where the temperature varies continuously with altitude. In the following, we consider  $I_s$  to be a constant throughout the cloud; the important consequences of (39) are well illustrated in this case.

#### Local thermodynamic equilibrium

If the gas of the cloud were in *complete thermodynamic equilibrium*, the radiation and matter would all be in thermal equilibrium at some temperature  $T$ ; the specific intensity  $I(\tau)$  would not vary throughout the cloud. In this case, the derivative in (39) equals zero,  $dI/d\tau = 0$ , and the observed intensity  $I(\tau)$  is given by

$$I(\tau) = I_s \quad \text{(Perfect thermal equilibrium)} \quad (11.40)$$

which is independent of  $\tau$ . Since  $I(\tau)$  is the specific intensity for complete thermodynamic equilibrium, its spectrum must be the Planck (blackbody) function (23). In turn, the source intensity  $I_s$  must also have a blackbody spectrum.

The solutions we seek are, in general, not for complete thermodynamic equilibrium because they involve a gas at one temperature and incoming photons representative of a slightly different temperature. Also, the limited extent of the cloud implies that radiation is leaving the volume of the cloud, so that complete equilibrium can not exist near the surface. Nevertheless, in solving the RTE one can make the assumption of *local thermodynamic equilibrium* (LTE).

Under LTE, the matter (e.g., protons and electrons) in a local region is in equilibrium with itself, but not necessarily with the radiation. That is, the matter obeys strictly the Boltzmann–Saha–Maxwell statistics, i.e., (9.14) and (9.15), for the local temperature, but the photon distribution is allowed to deviate slightly from it. Nevertheless, the radiation emitted from the local region follows the frequency dependence of the blackbody function for the local temperature, according to (40). The source function  $I_s$  for radiation emitted in a local region is therefore the blackbody function (23) for the (matter) temperature of the local region.

One can show that in the solar photosphere, the number density of particles is  $\sim 10^5$  times that of the photons. Since every such photon or particle has about the same energy,  $\sim kT$ , in thermal equilibrium, the energy content is overwhelmingly contained in the particles. They can thus maintain their own temperature and radiate at that temperature in their local region even if photons from a lower and slightly hotter region diffuse up into their region and minimally distort the overall photon spectrum.

#### Solution of the RTE

Insight into the behavior of  $I(\tau)$  according to the radiative transfer equation (39) can be gained simply from knowledge of the relative magnitudes of  $I(\tau)$  and  $I_s$ . If  $I(\tau) < I_s$  at some depth  $\tau$ , the derivative in (39) is positive which tells us that  $I(\tau)$  increases with optical depth. This is shown as the heavy line in Fig. 18a; note that it lies below the horizontal dashed line for  $I_s$ . Recall that in our case we hold  $I_s$  constant throughout the cloud. If, on the other hand,  $I(\tau) > I_s$ , then  $I(\tau)$  decreases with depth (heavy line in Fig. 18b). In each case,  $I(\tau)$  moves toward  $I_s$  and asymptotically approaches it at large optical depth.

At zero optical depth,  $I(0)$  is equal to the background intensity  $I_0$  because only the background source, and no part of the cloud, is in the observer's line of sight as is clear from Fig. 17. We also see this in both panels of Fig. 18. This obvious result also follows from the formal solution of the RTE to which we now proceed. We will find that the solution naturally provides for absorption and emission lines.



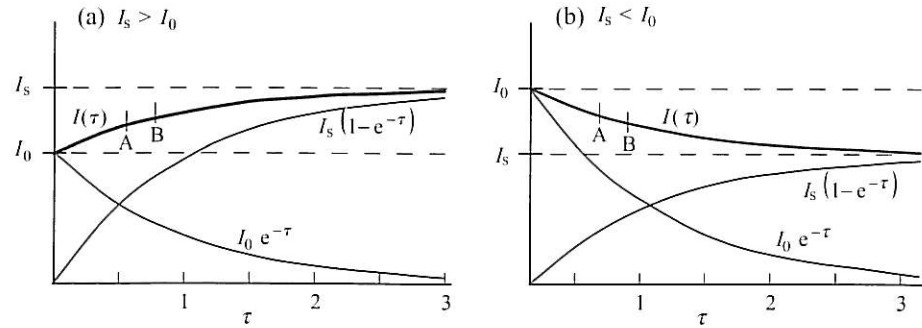


Figure 11.18. Plots of intensity  $I(\tau)$  vs. optical depth  $\tau$  from (44) for two cases: (a) source (cloud) intensity greater than the background intensity,  $I_s > I_0$ , and (b)  $I_s < I_0$ . As frequency is varied, the optical depth becomes higher at a resonance. If depth "A" is off resonance and depth "B" is centered at the resonance, case (a) yields an emission line and case (b) an absorption line.

The RTE (39) can be solved for  $I(\tau)$  by integration as follows. Multiply (39) by  $e^\tau$ ,

$$\frac{dI}{d\tau} e^\tau + I e^\tau = I_s e^\tau, \quad (11.41)$$

rewrite the left side as  $d(Ie^\tau)/d\tau$ , and integrate from 0 to  $\tau$ ,

$$\int_0^\tau d(Ie^\tau) = \int_0^\tau I_s e^\tau d\tau \quad (11.42)$$

For our cloud with  $I_s$  independent of optical depth  $\tau$ ,

$$I(\tau) e^\tau \Big|_0^\tau = I_s e^\tau \Big|_0^\tau \quad (11.43)$$

Insert the limits and divide through by  $e^\tau$ ,

$$\Rightarrow I(\tau) = I_0 e^{-\tau} + I_s(1 - e^{-\tau}) \quad (\text{Solution of radiative transfer equation}) \quad (11.44)$$

This is the solution of the RTE. The first term on the right shows the decreasing effect of the background radiation  $I_0$  as the optical depth increases, while the second term shows the increasing effect of the source (cloud) emission. These two terms and their sum are plotted in Fig. 18. These plots illustrate the variation of intensity with  $\tau$  for a single chosen frequency.

**Limiting cases**

The solution (44) readily illustrates the formation of spectral lines if we consider the variation of  $\tau$  (and also  $I_0$  and  $I_s$ ) with frequency. There are four cases to consider, one of which has two possibilities:

- $I_0 = 0$ : there is no background radiation illuminating the cloud
  - (i)  $\tau \ll 1$ : the gas is optically thin
  - (ii)  $\tau \gg 1$ : the gas is optically thick
- $I_0 > 0$ : background radiation illuminates the back of the cloud
  - (iii)  $\tau \ll 1$ : the gas is optically thin (for  $I_s > I_0$  and  $I_s < I_0$ )
  - (iv)  $\tau \gg 1$ : the gas is optically thick

*Case 1:  $I_0 = 0, \tau \ll 1$*

The condition  $I_0 = 0$  means that  $I(\tau)$  will be affected only by radiation from the cloud. The  $\tau \ll 1$  condition allows us to expand the exponential,  $e^{-\tau} \approx 1 - \tau$ . The solution (44) then reduces to

$$I(\tau) = \tau I_s \quad (I_0 = 0, \tau \ll 1) \quad (11.45)$$

This tells us that the emission is proportional to the optical depth, for  $\tau \ll 1$ . This is reasonable because, for an observer located at  $\tau \approx 0$  with leftward viewing detectors (Fig. 17), there are no atoms in view. The optical depth is zero and so is the detected intensity. As the observer moves to the right, toward increasing  $\tau$ , the number of atoms in the line of sight increases linearly with  $\tau$ . The cloud is optically thin so every layer  $d\tau$  of the cloud that is in view contributes equally to the intensity (Fig. 8.8); hence  $I \propto \tau$ . Note that changes in mass density  $\rho$  and opacity  $\kappa$  along the line of sight are automatically incorporated into  $\tau$ .

Now we address the frequency variation of the quantities in (45). Let the atoms in the cloud have an atomic transition or *resonance* at some frequency. At that frequency the cross section  $\sigma$  for absorption of incoming photons is high, and hence, so is the optical depth  $\tau$ . In general,  $\tau$  is a function of frequency and therefore so is the intensity  $I$ . We therefore rewrite (45) as

$$I(\nu) = \tau(\nu) I_s(\nu) \quad (I_0 = 0, \tau \ll 1) \quad (11.46)$$

Resonances at two distinct frequencies are hypothesized and illustrated in Fig. 19a (left panel) which is a plot of  $\tau$  vs.  $\nu$  for an observer at fixed position  $x$ . From (46), we see that high optical depths at these frequencies lead to high emerging fluxes  $I(\nu)$  at these same frequencies, provided that  $I_s$  is a smooth function of frequency. A plot of  $I$  vs.  $\nu$  for an arbitrarily chosen spectrum  $I_s(\nu)$  (Fig. 19a, right panel) shows emission lines at the two resonance frequencies. Note that the spectrum lies well below the source spectrum  $I_s$  because  $\tau \ll 1$ , in accord with (46).

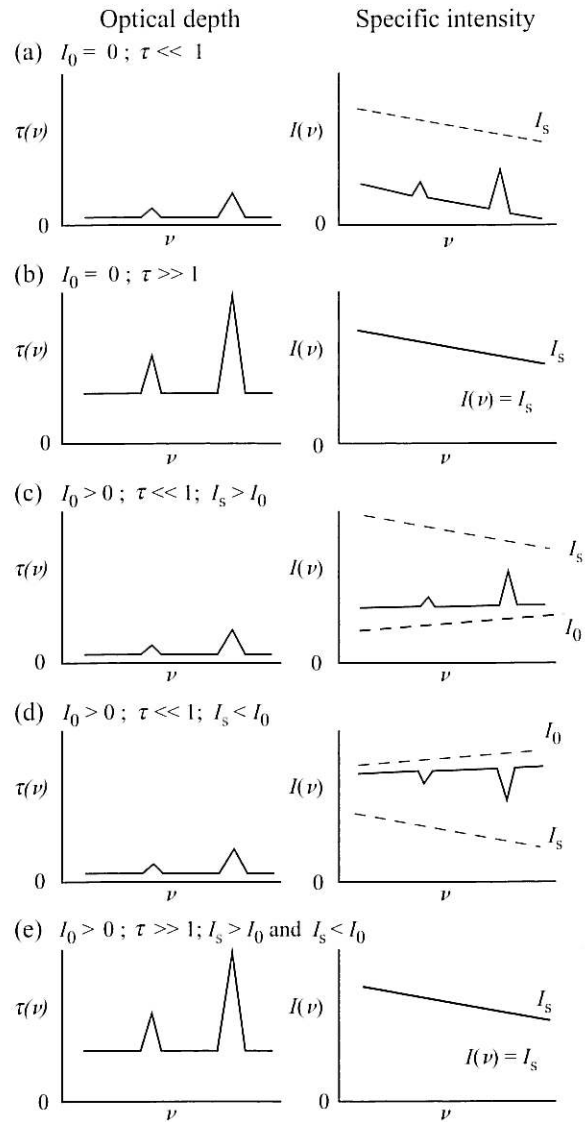


Figure 11.19. Frequency dependence of optical depth  $\tau(\nu)$  (left) and specific intensity  $I(\nu, \tau)$  (right) for an observer at some fixed position  $x$  in the cloud.  $I$  follows from  $\tau(\nu)$  and the solution (44) of the radiative transfer differential equation. Arbitrary spectral shapes for the source (cloud) spectrum  $I_s$  and the background spectrum  $I_0$  are shown as dashed lines. Emission lines are expected if the foreground gas is optically thin,  $\tau \ll 1$ , and hotter than the background source (c) or, in the limiting case, there is no background source (a). Absorption lines are expected if the background source is hotter than the foreground source, again if the cloud is optically thin (d). If the cloud is optically thick, the continuum spectrum of the cloud is observed (b,e).

At resonance frequencies, with their higher cross sections, the gas behaves as if it contains more atoms, or as if it were thicker. In this case, the observer would seem to “see” more emitting atoms, and hence greater intensity. At frequencies adjacent to a line,  $\tau$  will be lower by definition and fewer atoms are seen. If  $\tau$  is constant at these adjacent frequencies, as in the left panel of Fig. 19a, the output spectrum  $I(\nu)$  will, according to (46), mimic the spectrum  $I_s$  away from the line as shown in the right panel.

Case 2:  $I_0 = 0, \tau \gg 1$

Here the gas is very thick ( $\tau \gg 1$ ), and the expression (44) reduces to,

$$I(\nu) = I_s(\nu) \quad (I_0 = 0, \tau \gg 1) \quad (11.47)$$

which we have previously deduced (40); here we use the variable  $\nu$  rather than  $\tau(\nu)$ .

The output radiation given by (47) equals that of the continuum source specific intensity at all frequencies. If the source spectrum is the blackbody spectrum, the output spectrum at any depth  $\tau \gg 1$  is also blackbody. Even though the resonances may exist (Fig. 19b), the intensity  $I(\nu)$  has no dependence on  $\tau$ , and hence no spectral lines will form.

In this case, the local observer sees the maximum possible number of emitting atoms at any frequency so the resonances are not apparent. It is like being immersed in a thick fog that is denser (more opaque) in some directions than others. Nevertheless, the appearance in all directions (frequencies) is uniform as long as the fog is totally impenetrable ( $\tau \gg 1$ ) in all directions.

The observer in the fog sees only to a depth that yields enough water droplets to completely block the view. The same number of water droplets are thus seen in all directions, and the view appears uniform even though in some directions it penetrates less deeply than others. In our case, the increase of opacity at some frequency reduces the depth of view, but the observed intensity does not change.

The optically thick character of the gas allows the photons and particles to interact sufficiently to come into equilibrium thus giving rise to the continuum (blackbody) spectrum characteristic of the cloud.

Case 3:  $I_0 > 0, \tau \ll 1$

In this case, there is a source behind the cloud. Since  $\tau \ll 1$ , we again use the Taylor expansion,  $e^{-\tau} \approx 1 - \tau$ , so that (44) becomes

$$I = I_0 + \tau(I_s - I_0) \quad (I_0 > 0, \tau \ll 1) \quad (11.48)$$

Consider two cases here,  $I_s > I_0$  and  $I_s < I_0$ . In the former case, the output intensity is the background intensity  $I_0$  plus another positive term. If the optical depth  $\tau$  is higher at some frequency (i.e., greater opacity  $\kappa$ ) than at surrounding frequencies,

the emerging flux will be greater at that frequency. This yields an emission line (Fig. 19c).

In the case of  $I_s < I_0$ , the rightmost term is negative, and the emerging intensity is less than the background intensity. If again, the optical depth  $\tau$  is especially large at some frequency, the emerging intensity is depressed even more at that frequency. This yields an absorption line (Fig. 19d).

These same conclusions extend to somewhat larger optical depths,  $\tau \lesssim 2$ , as illustrated in the plots of the function  $I(\tau)$  vs.  $\tau$  (Fig. 18). In the case of  $I_s > I_0$  (Fig. 18a), the observed intensity  $I$  increases with optical depth  $\tau$ . At a given frequency not at a resonance, the intensity  $I$  might be given by the value at point A in the plot. At the frequency of a resonance, the optical depth is higher (by definition), and the observed intensity is therefore higher (point B). Thus an emission line is observed. For  $I_s < I_0$  (Fig. 18b), the increase in opacity again moves the observer from A to B, but in this case it yields a decrease in intensity, or an absorption line.

If the functions  $I_0$  and  $I_s$  are each blackbody spectra, the one with the higher temperature will have the greater intensity at any frequency (Fig. 8). Thus we have  $T_s > T_0$  for the  $I_s > I_0$  case, and  $T_s < T_0$  for the  $I_s < I_0$  case. We conclude therefore that if the temperature of the foreground cloud  $T_s$  is *greater* than the background temperature  $T_0$ , a spectrum with *emission lines* will emerge, and that if the cloud is *cooler* than the background, a spectrum with *absorption lines* will emerge.

In most stellar atmospheres at the depth seen in visible light (the photosphere), the temperature decreases with altitude, i.e., toward the observer. The deeper hot layers are then the background radiation for the higher, cooler regions. Absorption lines are thus prevalent in stellar spectra at visible wavelengths.

In contrast, radiation from the sun at ultraviolet frequencies yields emission lines. The observed ultraviolet radiation comes from high in the solar atmosphere because the higher opacities in the ultraviolet limit the depth into which the observer can "see". In these higher chromospheric regions, the temperature is increasing with height (moving toward the  $10^6$ -K corona). Thus the higher temperatures are in the foreground, and the spectra characteristically exhibit emission lines.

*Case 4:  $I_0 > 0$ ,  $\tau \gg 1$*

In this case, the gas is optically thick and (44) again yields

$$I(\nu) = I_s(\nu) \quad (11.49)$$

This is the same expression obtained when there was no background intensity (47). Since the gas is optically thick, the presence of the background source is immaterial (Fig. 19e). The radiation at any  $\tau$  is simply the continuum source (blackbody) spectrum of the optically thick cloud. It does not matter whether  $I_0 > I_s$  or  $I_0 < I_s$ .

### Summary

This concludes our discussion of the limiting cases of the solution to the radiative transfer equation. In each case the result is a continuum spectrum that reflects one or both of the spectra  $I_0$  and  $I_s$  with, in some cases, superimposed lines created by increases in the optical depth  $\tau$  at certain frequencies. If the foreground cloud intensity (temperature) is greater than the background intensity (temperature), emission lines are formed. If the opposite is true, absorption lines are formed.

### Problems

#### 11.2 Plots of spectra

*Problem 11.21.* (a) The spectral flux density in wavelength units of some source varies as the inverse fourth power of the wavelength,  $S_\lambda = K\lambda^{-4}$ , where  $K$  is a constant. What is  $S_\nu$ , expressed as a function of  $\nu$ ? See if you can do this from first principles without reference to the text. Give the units of  $S$  in both forms. (b) Develop an expression for the specific intensity in wavelength units,  $I_\lambda = I(\lambda, T)$ , for blackbody radiation. Start with the blackbody spectrum (23). Give the units of  $I_\lambda$ .

*Problem 11.22.* An x-ray astronomer measures the spectrum of the diffuse x-ray background over the range 2–60 keV and finds it to have an exponential shape. He reports the *energy* specific intensity to be

$$I_E = 3.6 \times 10^4 \exp\left(-\frac{h\nu}{23 \text{ keV}}\right) \text{ keV s}^{-1} \text{ m}^{-2} \text{ keV}^{-1} \text{ sr}^{-1}$$

where  $h\nu$  is given in keV. (a) Convert this to a *photon number* specific intensity  $I_p(\nu)$  with units  $\text{s}^{-1} \text{ m}^{-2} \text{ Hz}^{-1} \text{ sr}^{-1}$  and with the coefficient that gives the correct quantitative values. (b) This radiation is believed to come from the active galactic nuclei (AGN) of many distant galaxies, not from an isothermal optically thin plasma as might be inferred from its spectral shape; see Section 3. If it were such a plasma, what would be its temperature in kelvin? [Ans.  $\propto I_E/\nu$ ;  $\sim 10^8$  K]

#### 11.3 Continuum spectra

*Problem 11.31.* Consider the sketches of thermal bremsstrahlung spectra on a log-log plot in Fig. 3c. The curves are for two identical plasmas, with constant identical Gaunt factors, except that their temperatures differ. Suppose that one is three times hotter than the other,  $T_2 = 3T_1$ . (a) At what photon energy  $h\nu$  do the curves for  $T_1$  and  $T_2$  cross. Express your answer in terms of  $kT_1$ . (b) Make a quantitative log-log plot similar to Fig. 3c showing three thermal bremsstrahlung spectra ( $I$  vs.  $\nu$ ) for temperatures  $T$ ,  $2T$  and  $3T$ , drawn properly to scale, again for identical plasmas with identical constant Gaunt factors. [Ans. (a)  $\sim 0.8 kT_1$ ]



**Problem 11.32.** (a) Demonstrate that the Rayleigh–Jeans law (24) follows from the blackbody intensity (23) in the limit of low frequency. What is the condition on the frequency for this expression to be valid? (b) Find the temperature of the CMB radiation from the value of the fitted curve at 10 GHz in Fig. 9a. Would it have been easier to use Fig. 9b because the ordinate is a linear scale? Explain. [Ans. (b)  $\sim 3$  K]

**Problem 11.33.** (a) Write an expression for the radio portion of the spectrum  $I(\nu)$  of the Crab nebula as presented in Fig. 2. Give your answer in the forms  $S = K\nu^\alpha$  and  $S = K'(\nu/\nu_0)^\alpha$  where  $\nu_0$  is some convenient frequency (e.g., some integer power of 10) in the region. Hint: find the latter form first. Include numerical values for  $\alpha$ ,  $K$  and  $K'$ . (b) Repeat for the x-ray/gamma-ray portion of the spectrum. [Ans.  $\alpha \sim \nu^{-0.25}$ ;  $\alpha \sim \nu^{-1.5}$ ]

**Problem 11.34.** (a) Integrate graphically under the curve for the spectral flux density  $S$  given in Fig. 2 for the Crab nebula to find the flux density  $\mathcal{F}$  summed over all energy bands, from  $\log \nu = 6.5$  to  $\log \nu = 22.5$ . Take small slices along the abscissa, (one decade of frequency) to minimize errors due to the logarithmic scale. Interpolate over regions with no data. (b) The Crab nebula is  $\sim 6000$  LY distant. What is its luminosity, from  $10^{6.5}$  Hz to  $10^{22.5}$  Hz? Compare to the luminosity of the sun. (c) Comment on the relative fluxes in the several frequency bands, radio, optical, etc. [Ans.  $\sim 10^{31}$  W]

#### 11.4 Spectral lines

**Problem 11.41.** (a) What is the approximate equivalent width (in units of nm) of the prominent absorption line shown at  $\lambda \approx 485$  nm toward the left in Fig. 10a? (b) Estimate the equivalent width (in eV) of the Ne X emission line at  $\sim 1022$  eV in the Capella spectrum of Fig. 5. [Ans.  $\sim 1$  nm;  $\sim 100$  eV]

**Problem 11.42.** Calculate roughly the time for collisional de-excitation of a single oxygen (O III) atom in a metastable state if it resides in an emission nebula (H II region). The de-excitations take place because fast electrons collide with the relatively large and slow oxygen atom. The approximate time between collisions is the required answer. Let the density of electrons in the nebula be  $n = 1 \times 10^8 \text{ m}^{-3}$ , the temperature of the electrons be  $T \approx 7000$  K, and the size (diameter) of the oxygen atom be  $d \approx 0.3$  nm. Compare your answer to the natural or spontaneous decay time of  $\sim 100$  s for the metastable states of Table 1 (assuming no collisions). Hints: (i) Consider the size of the electron to be negligible when estimating the cross section for the collision. (ii) The speed of the electron may be obtained from the relation  $3kT/2 = mv^2/2$ . (iii) The oxygen atom may be considered to be a stationary target (why?). [Ans.  $\sim 3$  days]

**Problem 11.43.** (a) For the damping profile (30), find the frequency where the maximum amplitude occurs, the value of  $\kappa_1/\kappa_{1,0}$  at this frequency, and  $(\nu - \nu_0)_{\text{HM}}$ ,

the half width of the curve at one-half the maximum amplitude (HWHM). (b) Based on these results, make rough sketches of the damping curves for  $\gamma = 0.5, 1$ , and 2. (c) Repeat part (a) for the Doppler distribution (28). (d) Consider Fig. 15. What is the value of the parameter  $\gamma$  for the damping expression given there? Find an expression for the Doppler response  $\kappa_1$  that has unit amplitude and HWHM twice that of the HWHM of the damping curve. Compare to the Doppler expression given in the figure. [Ans.  $\nu_0, 4/\gamma, \gamma/2$ ; —;  $\nu_0, 1, \sigma(2 \ln 2)^{1/2}$ ; 1, same]

#### 11.5 Formation of spectral lines (radiative transfer)

**Problem 11.51.** Consider a stellar atmosphere where  $I_s$  varies with depth in the cloud as  $I_s = a + b\tau$  where  $a$  is a positive constant and  $b$  is a constant that can be positive or negative. (In the text, we took  $I_s$  to be constant throughout the cloud.) Assume that conditions of local thermodynamic equilibrium are satisfied, and that the observer views the atmosphere head on, as in Fig. 17. (The variation in  $I_s$  arises through a variation the volume emissivity with position (38) which in turn is a consequence of temperature variation within the atmosphere. (a) Find the solution  $I(\tau)$  of the equation of radiation transfer (39) for this situation. (b) Evaluate the solution for the case of no background source,  $I_0 = 0$ , with  $\tau \ll 1$  and with  $\tau \gg 1$ . (c) Explain why spectral lines will or will not be formed in each of these two cases. If they are, what are the condition(s) on  $b$  that result in emission or absorption lines? In the  $\tau \ll 1$  case, how would you constrain  $b$  so that only emission lines occur in the region  $\tau < 0.1$ , in the context of your approximations? [Ans. (b)  $I(\tau \ll 1) \approx a\tau + (b - a)(\tau^2/2)$ ]